Progress In Electromagnetics Research C, Vol. 45, 163–178, 2013

NUMERICAL AND EXPERIMENTAL ANALYSIS OF WIDEBAND E-SHAPED PATCH TEXTILE ANTENNA

Hai Sheng Zhang*, Shun Lian Chai, Ke Xiao, and Liang Feng Ye

College of Electronic Science and Engineering, National University of Defense Technology, Changsha 410073, China

Abstract—In this paper, we present a wideband planar E-shaped textile antenna and study its performance numerically and experimentally. The textile material and radiation patch shape provide the antenna a wide working band (2.25 GHz–2.75 GHz). A digital human model is established to numerically analyze the affect of human body on antenna. Experiments are carried out to study the performance changes of antenna in different states which may be experienced in the potential applications. These states are antenna on human body, antenna getting bent, and antenna after getting wet. The simulated and measured results in free space and on human chest show good agreement with each other. From the study it is also found that the textile antenna's performance does not get deteriorated in these states. Therefore, the wideband planar E-shaped textile antenna is suitable for body-centric wireless communications with high quality.

1. INTRODUCTION

With the development of body-centric wireless communications [1–5], more and more communications systems contain antennas integrated in clothing, called wearable antennas [6–9]. Wearable antennas are mainly divided into three types, hard dielectric substrate antenna with low profile and small area [10–12], flexible antenna with substrate of foam or flexible PCB (printed circuit board) [13–17], and textile antenna [18–23]. Hard dielectric substrate antennas are usually restricted by antenna area and antenna form, and operating bandwidth is often difficult to achieve the requirement. Flexible antennas with substrate

Received 13 September 2013, Accepted 13 November 2013, Scheduled 18 November 2013
* Corresponding author: Hai Sheng Zhang (hsh_zhang@163.com).

of foam or flexible PCB are difficult to be integrated well with clothing, and the area of the antenna cannot be too large. Textile antenna means that the conductive or non-conductive material of antenna adopts fabric material. This type can be well integrated with clothes and is not restricted by the antenna area, which can bring more freedom to design, so it has the most potential for wearable antennas. There are several papers focusing on textile patch antenna. Hertleer et al. presented a aperture-coupled method [24] for textile antenna feed, and Locher et al. adopted direct edge feed method [25]. The two methods have to use textile microstrip line inevitably, which increases the possibility of interference from the human body, and the textile microstrip line needs to be connected to coaxial via SMA connector eventually, which also brings instability to the feed. Actually, probe feed may be a better choice for textile patch antennas before the more advanced textile transmission technology appears. This paper will adopt probe feed method for textile patch antenna.

The design and manufacture difficulties of textile antenna are as follows: 1) Compared to lithography printed antenna, the manufacture accuracy of textile antenna is very low. 2) The shape change of textile antenna is unpredictable, which may lead to a drift of work-band and deterioration of radiation performance. 3) The antenna is located in the proximity of human body, which may have a greater impact on the antenna. Therefore, the requirements of a good textile antenna are low demand for manufacture accuracy, wide band, and insensitive to human body. Based on the above analysis. This paper presents a wideband E-shaped patch textile antenna to meet the above requirements. Compared to other forms of patch antenna, E-shaped structure is relatively simple and easy to manufacture. The size of the antenna is large enough to reduce dimensional accuracy requirement. The work-band of E-shaped patch textile antenna is 2.25 GHz–2.75 GHz, which covers the 2.45 GHz ISW band and the work-band of the forth generation mobile system in China: Time Division Long Term Evolution (TD-LTE). From the plan of Ministry of Industry and Information Technology, the band of 2.32 GHz–2.37 GHz is used for TD-LTE coverage indoor, and the band of 2.57 GHz–2.62 GHz is used for TD-LTE coverage outdoor. The antenna bandwidth is about 20% with a center frequency of 2.5 GHz. So even the working band of the antenna drifts. The antenna can also work at some required frequency, and the shielding effect of the antenna ground reduces the body effect on antenna.

The antenna is located in proximity of human body, so it is necessary to consider the interaction between the human body and the antenna [26–30]. Finite-difference time-domain (FDTD) method is

a direct time-domain method to solve Maxwell's Equations [31], which is suitable for dealing with the complex and highly inhomogeneous human body. However, a high spatial resolution is often required for the description of the antenna's small geometrical features. Therefore, considering the size of human body and a uniform meshing for the whole FDTD domain, the human body will be a large oversampling area, and the computation time and memory requirements will increase greatly. For such a multi-scale problems, a numerical technique based on the surface equivalence theorem is adopted to characterize on-body antennas [32]. This method divides the original problem into two sub-problems, each characterized by a different mesh. Then the equivalent principle is used on the surface of two sub-problems to reduce the reflection from interface. Hence, for the first, this paper adopts equivalent principle FDTD method to analyze the wearable antenna with an accurate human digital model [33].

The rest of this paper is organized as follows. Section 2 shows a wideband planar E-shaped textile antenna and introduces a numerical analysis method. Section 3 presents some numerical results and their comparison with measurement in different states. Section 4 draws a conclusion.

2. ANTENNA DESIGN AND NUMERICAL METHOD

2.1. Antenna Design and Prototyping

In order to design a patch textile antenna, a selection of suitable conducting and non-conducting textile materials is required. Conducting material is applied to both the patch and the ground plane, while non-conducting textile is needed for the antenna substrate layer. For the antenna substrate, a fleece fabric is chosen because of its high thickness and a low permittivity of 1.14, which are excellent properties for textile antenna design. The three fleece fabric layers are stitched together in order to ensure a well-defined substrate thickness and to keep the antenna conformal when it is bent, which has a thickness of 10 mm and provides an adequate antenna bandwidth. The conducting material is self-adhesive copper foil tape from Shenzhen JUNYE Inc., which has a thickness of 0.035 mm and provides low surface resistivity $\mathrm{Rs} < 0.03\,\Omega/\mathrm{sq}$. The self-adhesive side makes it easy to fasten the copper tape to the substrate. This conducting material is chosen also because of its easy handling such as cutting and sewing.

Since the E-shaped patch antenna was proposed by Yang et al. in 2001 [35], various forms of improved E-shaped patch antenna have appeared successively. Salonen et al. presented a dual-band E-shaped patch wearable textile antenna [36] in 2005, which worked at a double

resonant frequencies of 2.2 GHz and 3.0 GHz. We makes the two resonant frequencies closer to form a continuous work-band of 2.25–2.75 GHz by adjusting the design parameters of the E-shaped patch antenna. The two resonant frequencies are still visible at 2.38 GHz and 2.54 GHz, shown in Figure 5. The single-feed planar E-shaped textile antenna works for short range wireless communication and personal area networks. As shown in Figure 1, the reasonable size and simple shape reduce the difficulty of processing of the textile antenna. Actually, we have made several textile antennas. The manual processing errors did not have a significant impact on antenna performance, which shows that the objective of reducing the sensitivity on the machining accuracy is achieved by rational designing of antenna size.

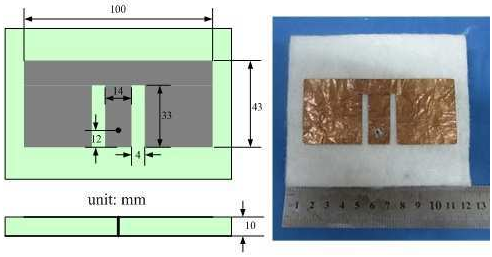

Figure 1. Geometry of planar E-shaped textile antenna.

2.2. Description of the Numerical Method

Consider the problem presented in Figure 2. As it is shown in this figure, the antenna is located in proximity of human body. For such a multi-scale problems, the simulation is divided into two FDTD simulations steps.

The aim of the first step of the equivalent principle FDTD is recording antenna's primary radiation by the use of an excitation recording surface placed around it. Thus the antenna is described using a fine mesh to describe its geometrical features. Absorbing boundary condition is adopted to simulate the infinite open space. The field components on the excitation recording surface are recorded in a data file for every time step. These records will be used as the excitation of the next step of equivalent principle FDTD. This step starts at t_0 and ends at t_1 when all the electromagnetic energy radiates outside the excitation recording surface.

The calculation region of the second step of the equivalent principle FDTD contains the whole problem of both the antenna and

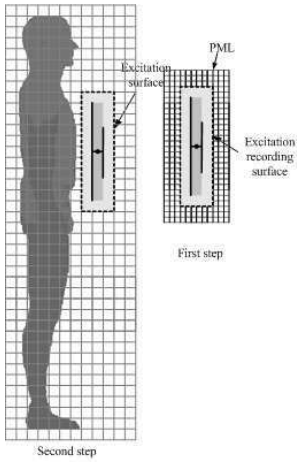

Figure 2. Equivalent principle FDTD principle.

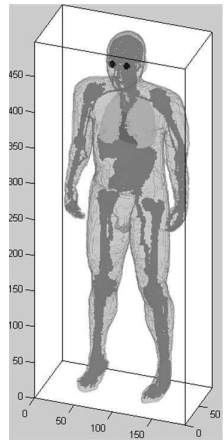

Figure 3. Zubal human digital phantom.

the human body. It aims at calculating the antenna radiation while taking into account the coupling effect between the antenna and the human body. The whole region is described using a coarse mesh to reduce memory requirement. Absorbing boundary condition located outside the whole region is adopted to calculate the antenna radiation. The field components recorded in the first step are used as excitation source in this step, which is realized by using the total-field/scattered-field boundary condition on the excitation surface to ensure that only scattered-field exists inside the excitation surface. This step starts at t_0 and ends at t_2 generally longer than t_1 to allow the electromagnetic energy radiates outside the whole region. The Mesh density of the second step is chosen in order to correctly represent the human body, but it only provides a coarse description of the antennas. More specifically, it is not fine enough to simulate the antenna radiation in the first step, but it is just enough to simulate the reflected signal received by the antenna in the second step.

Since grid density and time step are inconsistent in the two steps, an interpolation process of the field component recorded in the first step is needed before it is used as excitation source in the second step. It is a fine-to-coarse interpolation process. The spatial interpolation can be realized by weighted average of the electromagnetic fields of neighboring grids, and the temporal interpolation can be realized by weighted average of the electromagnetic fields of adjacent time.

The next is post processing. After the above two steps, we

Table 1. Permittivity and conductivity of human tissues at 2.5 GHz.

Tissue	ε_r	σ (S/m)
Skin Dry	38.063	1.4407
Brain White Matter	36.226	1.1899
spinal cord	30.196	1.0681
Bone Cancellous	18.606	0.78761
Muscle	52.791	1.705
Lung Inflated	20.51	0.79022
Heart	54.918	2.2159
Liver	43.118	1.6534
Gall Bladder	57.68	2.023
Kidney	52.856	2.3901
Cartilage	38.878	1.7172
Oesophagus	62.239	2.1671
Stomach	62.239	2.1671
Small Intestine	54.527	3.1335
Colon	53.969	1.9997
Pancreas	57.272	1.9283
Fat	5.2853	0.10235
Blood	58.347	2.5024
Bone Marrow	5.3024	0.092834
Lymph	57.272	1.9283
Thyroid	57.272	1.9283
Trachea	39.79	1.4206
Spleen	52.546	2.2
Testis	57.629	2.1273
Prostate	57.629	2.1273
Duodenum	62.239	2.1671
Mucous Membrane	42.923	1.5618
Cerebellum	44.893	2.069
Tongue	52.698	1.7662
Lens	44.681	1.4738
Tooth	11.41	0.38459

can calculate the reflection coefficient S_{11} and the antenna radiation pattern. S_{11} is calculated as follows:

$$S_{11} = \frac{V_{tot}(f) - Z_0 I_{tot}(f)}{V_{tot}(f) + Z_0 I_{tot}(f)} \quad (1)$$

$$V_{tot}(t) = V_{\text{step}\,1}(t) + V_{\text{step}\,2}(t) \quad (2)$$

$$I_{tot}(t) = I_{\text{step}\,1}(t) + I_{\text{step}\,2}(t) \quad (3)$$

where $V_{tot}(f)$ and $I_{tot}(f)$ are the Fourier transform of the corresponding voltage $V_{tot}(t)$ and current $I_{tot}(t)$ of the feeding point. The $V_{tot}(t)$ and $I_{tot}(t)$ are the sums of the simulation results of the two steps. Radiation pattern calculation is completed in the second step, which is the same as the conventional FDTD method.

In order to accurately predict the effect of the human body on antenna, the human model should be as accurate as possible. This paper adopts Zubal Phantom data [33], which is established based on computer tomography (CT) and magnetic resonance imaging (MRI) data of two living human males. It is segmented into 88 different organ types, and the resolution of Zubal Phantom data is $3.6 \times 3.6 \times 3.6\,\text{mm}^3$. Three-dimensional human model is shown in Figure 3. In order to show clearly, it draws only brain, eyes, bones, and stomach. In order to simulate conveniently, the 88 different organ types are attributed to 31 kinds of tissue types, The permittivity and conductivity [34] for the 31 tissues at 2.5 GHz are shown in Table 1.

3. NUMERICAL AND EXPERIMENTAL RESULTS

In this section, we first compare the simulated and measured results of the antenna in free space and onbody and show the input reflection coefficient and radiation pattern of the antenna. Secondly, we carry out measurements with the antenna bent around cylinder and bent on human arm in order to investigate their potential behavior in wearable applications. Finally, we carry out measurements to study the antenna performance changes after getting wet, because this state may appear in wearable applications.

3.1. Antenna in Free Space and on Human Chest

The antenna reflection coefficients were measured using an HP 8510 Vector Network Analyzer, and the antenna radiation patterns were measured in the microwave anechoic chamber. The antenna location on the humanbody is show in Figure 4, which is placed in center of the body, about 20 cm under the shoulder, and the antenna ground is about 1 cm from the body surface.

Figure 4. Antenna location on human chest.

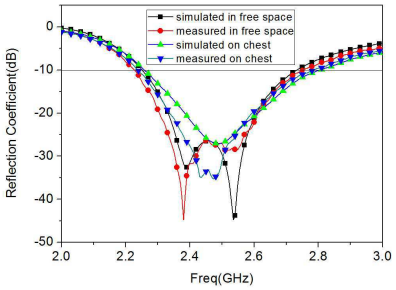

Figure 5. Comparison of the reflection coefficients of antenna in free space and on human chest.

It can be noticed that the simulated and measured results in free space show good agreement with each other in Figure 5. The results show the good impedance matching across the bandwidth of 2.25 GHz–2.75 GHz for the −10 dB reflection coefficient, featuring 20% bandwidth with a center frequency of 2.5 GHz. The simulated and measured results on human chest are consistent with each other. The difference between the two is because the simulation method and simulation model are not precise enough, and the measurement and simulation models cannot be fully consistent with each other. By comparing the antenna performance in free space and on human body, we can see that the presence of the human body acts as a load and slightly affects the impedance matching. The change in reflection coefficient can be due to both the impedance matching and the power absorption by the human body. Due to the isolation effect of the antenna's ground, the effect of human body on antenna is very small, which is also consistent with our design expectations.

Figure 6 shows the distribution of the radiation pattern in free space and around the human chest in the horizontal plane at 2.3, 2.5, and 2.7 GHz. It is clear that the measurements agree well with the simulation results. We observe only small differences. The measured gain is about 2 dB lower than the simulated result, because the actual antenna efficiency is less than the lossless simulated antenna, which is probably caused by manufacturing imperfections and material loss. The measured gains in free space are between 8 dB and 9 dB, which is similar to the results in [24]. When comparing the radiation patterns in free space and on human chest, we find the shielding effect provided from the metallic ground plane minimizes the absorption of the energy

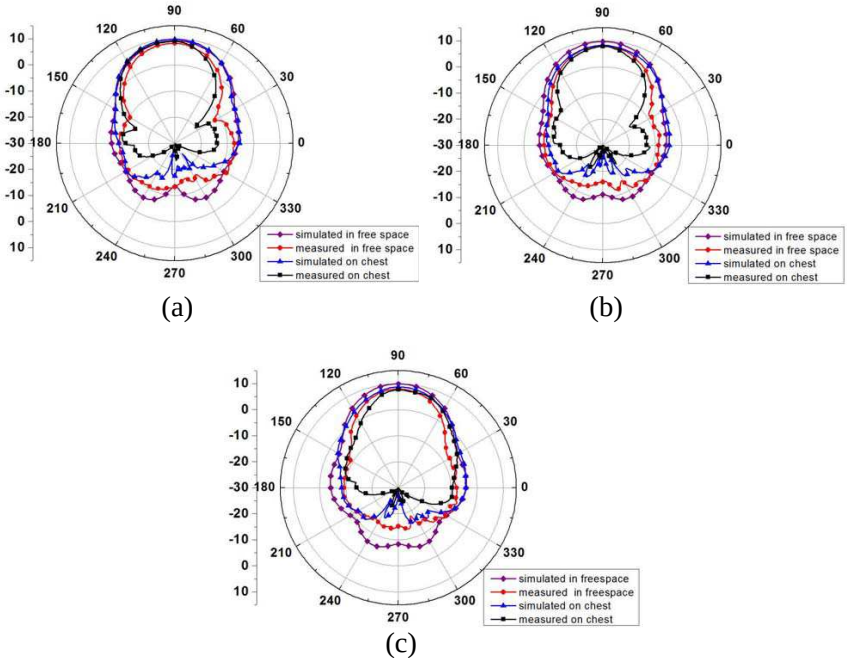

Figure 6. Comparison of the radiation patterns of antenna in free space and on human chest. (a) 2.3 GHz. (b) 2.5 GHz. (c) 2.7 GHz.

by the human body, and hence, the radiation pattern is slightly distorted from that in free space. The result indicates that the use of planar E-shaped textile antenna with a ground plane for body-centric communications minimizes the effect of human body on antenna.

3.2. Bending Effect on Textile Antenna

In the case of potential applications, the antenna may be in the bent state, so we studied its effect on planar E-shaped textile antenna. In Figure 7, the antenna is fixed to a cylinder with a diameter of 12 cm, and the bending gauge must not affect the measured antenna characteristic, so we chose foam (dielectric constant about 1) and dug round hole in the center for antenna feeding. Next, we carried out measurements to study the antenna performance changes bent on human arm. A 10 mm foam gap is postulated between the antenna ground plane and the human arm.

In Figure 8, the reflection coefficient in flat state is compared to the results in bent state and on human arm. It is clear that the working

Figure 7. Antenna location on foam cylinder and on the human arm.

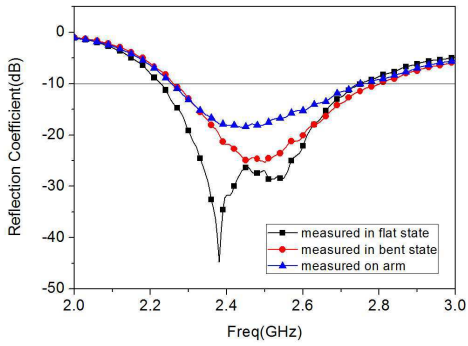

Figure 8. Comparison of the reflection coefficients of antenna in flat and bent states.

band in bent state shifts upward about 50 MHz compared with the flat state, and bandwidth on human arm is reduced about 50 MHz. The magnitude of reflection coefficient offsets about 5 dB and 10 dB for bending in free space and on human arm, respectively. This behavior can be seen best at a frequency of 2.5 GHz in Figure 8. Nevertheless, the antenna shows good impedance matching across the bandwidth of 2.3 GHz–2.75 GHz for the −10 dB reflection coefficient. So it can be concluded that a robust design is obtained by extending the bandwidth to 2.25–2.75 GHz, to accommodate the potential shift in frequency or the deterioration of reflection coefficient in a real-life application. The same results are shown in [37, 38], and they had found that bending would decrease the antenna's bandwidth and made it shift upward.

Figure 9 shows the radiation pattern in flat state, bent state and on human arm in the horizontal plane at 2.3, 2.5, and 2.7 GHz. We can

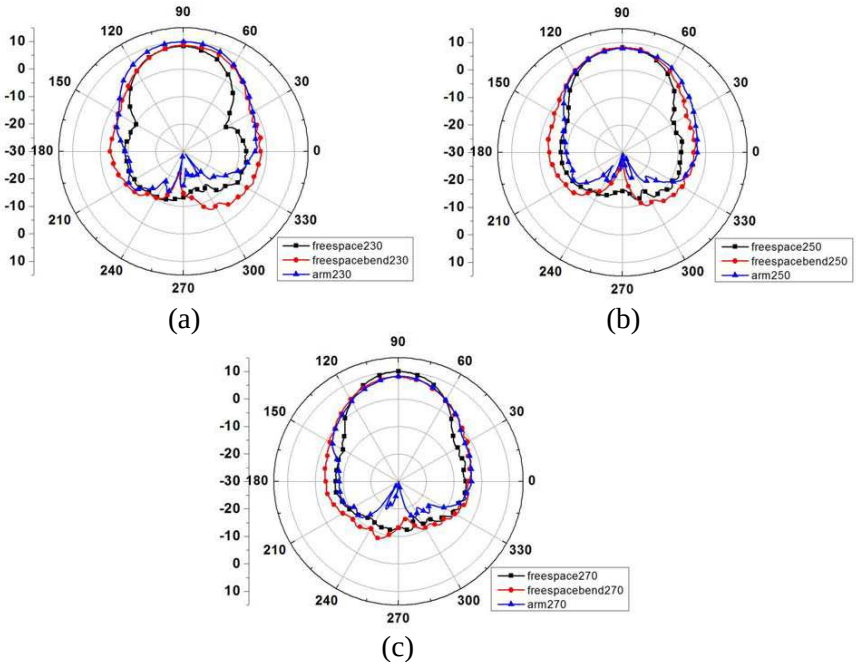

Figure 9. Comparison of the radiation pattern of antenna in flat and bent states. (a) 2.3 GHz. (b) 2.5 GHz. (c) 2.7 GHz.

see that the bent antenna patterns are less directional for both bent states compared to its patterns in flat shape, which is reflected in the wider lobe pattern in the main radiation direction. Besides, because of the shielding effect of human body, the back radiation on human arm remains about 10 dB smaller than the other states. Nevertheless, the shape of the radiation pattern, and the gain of the antenna changes slightly, due to relatively large area of the antenna. The result indicates that bending the antenna has little effect on the radiation pattern of this planar E-shaped textile antenna.

3.3. Dry-wet-dry Changing Effect on Textile Antenna

As part of the wearable system, the textile antennas are likely to experience getting wet and then drying process. In the dry-wet-dry again changing process, the deformation of the fabric will bring unexpected impact on antenna performance. So we carried out measurements to study the antenna performance changes in the dry-wet-dry again changing process. In this paper, the substrate material

Figure 10. Textile antenna in water.

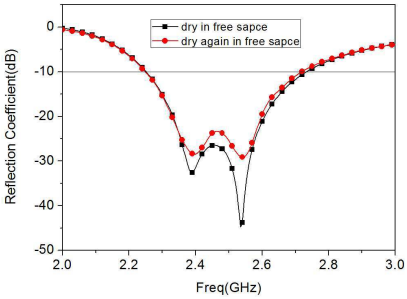

Figure 11. Comparison of the reflection coefficients of antenna in dry and dry-again states.

of antenna is fleece fabric, which is not a waterproof material, so it can be expected that the permittivity will change significantly in the wet state. This may bring very negative impact on antenna performance. In Figure 10, we keep the textile antenna in water for several minutes to ensure that it is completely soaked.

The reflection coefficient of antenna in wet state is almost 0 dB across the whole working band, which is the same as that we have inferred. This is mainly because the permittivity of substrate is completely changed in wet state. Figure 11 just compares the reflection coefficient of antenna in dry and dry-again states. It can be noticed that the measured results in dry and dry-again states show good agreement with each other. This means that although the fleece fabric is not a waterproof substrate material, it still keep stability in size and permittivity in dry and dry-again states.

4. CONCLUSION

We present a wideband planar E-shaped textile antenna and study its performance numerically and experimentally. The agreement of simulated and measured results shows that the analysis method and experimental results are accurate and effective. The antenna not only has good properties, but also is easy to manufacture. It satisfies communication requirements even when placed on human chest and bent on human arm. Furthermore, the antenna provides sufficient antenna gain to be applied in a body-centric wireless communications.

ACKNOWLEDGMENT

The authors would like to thank Mr. Ke Xiao for the assistance in the antenna measurements. The authors would also like to thank G. Zubal, for the providing of human digital model and G. Camelia, for the providing of electromagnetic parameters of human tissue.

REFERENCES

1. Hall, P. S. and Y. Hao, *Antennas and Propagation for Body-centric Wireless Communications,* Artech House, 2006.
2. DiBari, R., Q. H. Abbasi, A. Alomainy, and Y. Hao, "An advanced UWB channel model for body-centric wireless networks," *Progress In Electromagnetics Research*, Vol. 136, 79–99, 2013.
3. Chahat, N., C. Leduc, M. Zhadobov, and R. Sauleau, "Antennas and interaction with the body for body-centric wireless communications at millimeter-waves," *2013 7th European Conference on Antennas and Propagation (EuCAP)*, 772–775, 2013.
4. Osman, M. A. R., M. K. A. Rahim, N. A. Samsuri, H. A. M. Salim, and M. F. Ali, "Embroidered fully textile wearable antenna for medical monitoring applications," *2013 7th European Conference on Antennas and Propagation (EuCAP)*, 777–781, 2013.
5. Liu, Z. G. and Y. X. Guo, "Dual band low profile antenna for body centric-communications," *IEEE Transactions on Antennas and Propagation*, Vol. 61, No. 4, 2282–2285, 2013.
6. Scarpello, M. L., I. Kazani, C. Hertleer, H. Rogier, and D. Vande-Ginste, "Stability and efficiency of screen-printed wearable and washable antennas," *IEEE Antennas and Wireless Propagation Letters*, Vol. 11, 838–841, 2012.
7. Serra, A. A., P. Nepa, and G. Manara, "A wearable two-antenna system on a life jacket for Cospas-Sarsat personal locator beacons," *IEEE Transactions on Antennas and Propagation*, Vol. 60, No. 2, 1035–1042, 2012.
8. Koski, K., A. Vena, L. Sydanheimo, L. Ukkonen, and Y. Rahmat-Samii, "Design and implementation of electro-textile ground planes for wearable UHF RFID patch tag antennas," *IEEE Antennas and Wireless Propagation Letters*, Vol. 12, 964–967, 2013.
9. Chahat, N., M. Zhadobov, L. Le Coq, and R. Sauleau, "Wearable endfire textile antenna for on-body communications at 60 GHz,"

IEEE Antennas and Wireless Propagation Letters, Vol. 11, 799–802, 2012.

10. Pitra, K. and Z. Raida, "Miniaturized antenna for body centric communication," *2013 7th European Conference on Antennas and Propagation (EuCAP)*, 3219–3222, 2013.
11. SanzIzquierdo, B., J. A. Miller, J. C. Batchelor, and M. I. Sobhy, "Dual-band wearable metallic button antennas and transmission in body area networks," *IET Microwaves, Antennas and Propagation*, Vol. 4, No. 2, 182–190, 2010.
12. Sabban, A., "New wideband printed antennas for medical applications," *IEEE Transactions on Antennas and Propagation*, Vol. 61, No. 1, 84–91, 2013.
13. Raad, H. R., A. I. Abbosh, H. M. Al-Rizzo, and D. G. Rucker, "Flexible and compact AMC based antenna for telemedicine applications," *IEEE Transactions on Antennas and Propagation*, Vol. 61, No. 2, 524–531, 2013.
14. Kim, S., Y. J. Ren, H. Lee, A. Rida, S. Nikolaou, and M. M. Tentzeris, "Monopole antenna with inkjet-printed EBG array on paper substrate for wearable applications," *IEEE Antennas and Wireless Propagation Letters*, Vol. 11, 663–666, 2012.
15. Osman, M. A. R., M. K. A. Rahim, N. A. Samsuri, H. A. M. Salim, and M. F. Ali, "Embroidered fully textile wearable antenna for medical monitoring applications," *Progress In Electromagnetics Research*, Vol. 117, 321–337, 2011.
16. Vladimir, H., "Planar antenna in proximity of human body models," *2013 7th European Conference on Antennas and Propagation (EuCAP)*, 3309–3311, 2013.
17. Ehteshami, N., V. Sathi, and M. Ehteshami, "Experimental investigation of a circularly polarised flexible polymer/composite microstrip antenna for wearable applications," *IET Microwaves, Antennas and Propagation*, Vol. 6, No. 15, 1681–1686, 2012.
18. Hertleer, C., H. Rogier, L. Vallozzi, and L. V. Langenhove, "A textile antenna for off-body communication integrated into protective clothing for fire fighters," *IEEE Transactions on Antennas and Propagation*, Vol. 57, No. 4, 919–925, Apr. 2009.
19. Osman, M. A. R., M. K. A. Rahim, N. A. Samsuri, H. A. M. Salim, and M. F. Ali, "Embroidered fully textile wearable antenna for medical monitoring applications," *Progress In Electromagnetics Research*, Vol. 117, 321–337, 2011.
20. Kamardin, K., M. K. Abd Rahim, N. A. Samsuri, M. E. B. Jalil,

and I. H. Idris, "Textile artificial magnetic conductor waveguide jacket for on-body transmission enhancement," *Progress In Electromagnetics Research B*, Vol. 54, 45–68, 2013.

21. Sankaralingam, S. and B. Gupta, "Development of textile antennas for body wearable applications and investigations on their performance under bent conditions," *Progress In Electromagnetics Research B*, Vol. 22, 53–71, 2010.
22. Soh, P. J., S. J. Boyes, G. A. E. Vandenbosch, Y. Huang, and S. L. Ooi, "On-body characterization of dual-band all-textile PIFA," *Progress In Electromagnetics Research*, Vol. 129, 517–539, 2012.
23. Sankaralingam, S. and B. Gupta, "Experimental results on HiperLAN/2 antennas for wearable applications," *Progress In Electromagnetics Research C*, Vol. 25, 27–40, 2012.
24. Hertleer, C., A. Tronquo, H. Rogier, L. Vallozzi, and L. Van Langenhove, "Aperture-coupled patch antenna for integration into wearable textile systems," *IEEE Antennas and Wireless Propagation Letters*, Vol. 6, 392–395, 2007.
25. Locher, I., M. Klemm, T. Kirstein, and G. Troster, "Design and characterization of purely textile patch antennas," *IEEE Transactions on Advanced Packaging*, Vol. 29, No. 4, 777–788, 2006.
26. Koohestani, M., N. Pires, A. K. Skrivervik, and A. A. Moreira, "Performance study of a UWB antenna in proximity to a human arm," *IEEE Antennas and Wireless Propagation Letters*, Vol. 12, 555–558, 2013.
27. Klemm, M. and G. Troester, "EM energy absorption in the human body tissues due to UWB antennas," *Progress In Electromagnetics Research*, Vol. 62, 261–280, 2006.
28. Kong, L. Y., J. Wang, and W. Y. Yin, "A novel dielectric conformal FDTD method for computing SAR distribution of the human body in a metallic cabin illuminated by an intentional electromagnetic pulse," *Progress In Electromagnetics Research*, Vol. 126, 355–373, 2012.
29. Jalil, M. E. B., M. K. Abd Rahim, N. A. Samsuri, N. A. Murad, H. A. Majid, K. Kamardin, and M. Azfar Abdullah, "Fractal Koch multiband textile antenna performance with bending, wet conditions and on the human body," *Progress In Electromagnetics Research*, Vol. 140, 633–652, 2013.
30. Liu, Y., Z. Liang, and Z. Q. Yang, "Computation of electromagnetic dosimetry for human body using parallel FDTD algorithm combined with interpolation technique," *Progress In*

Electromagnetics Research, Vol. 82, 95–107, 2008.

31. Taflove, A., *Computational Electrodynamics: The Finite Difference Time Domain Method,* Artech House, 1995.
32. Miry, C., R. Loison, and R. Gillard, "An efficient bilateral dual-grid-FDTD approach applied to on-body transmission analysis and specific absorption rate computation," *IEEE Transactions on Microwave Theory and Techniques*, Vol. 58, No. 9, 2375–2382, 2010.
33. Zubal, G., C. Harrell, and E. Smith, "Zubal phantom data," Yale University School of Medicine, New Haven, CT USA, http://noodle.med.yale.edu/.
34. Camelia, G. and G. Sami, "Compilation of the dielectric properties of body tissue at RF and microwave frequencies," Italian National Research Council Institute for Applied Physics Research, http://niremf.ifac.cnr.it/tissprop/htmlclie/htmlclie.htm.
35. Yang, F., X. X. Zhang, X. Ye, and Y. Rahmat-Samii, "Wide band E-shaped patch antenna for wireless communications," *IEEE Transactions on Antennas and Propagation*, Vol. 49, No. 7, 1094–1100, 2001.
36. Salonen, P., K. Jaehoon, and Y. Rahmat-Samii, "Dual-band E-shaped patch wearable textile antenna," *The Antennas and Propagation Society International Symposium*, Vol. 1, 466–469, 2005.
37. Tronquo, A., H. Rogier, C. Hertleer, and L. Van Langenhove, "Robust planar textile antenna for wireless body LANs operating in 2.45 GHz ISM band," *Electronics Letters*, Vol. 42, No. 3, 142–143, 2006.
38. Kaivanto, E. K., M. Berg, E. Salonen, and P. de Maagt, "Wearable circularly polarized antenna for personal satellite communication and navigation," *IEEE Transactions on Antennas and Propagation*, Vol. 59, No. 12, 4490–4496, 2013.